The Effect of Cold Rolling Parameters on the Recrystallization Texture of Non-Oriented Electrical Steel

R. Kawamata, T. Kubota, and K. Yamada

The effect of cold rolling condition on magnetic properties of non-oriented electrical steel was investigated. For evaluation of cold rolling condition, utilizing rolling shape factor (RSF) was proposed. In the case of small RSF, magnetic induction was improved. Development of ND || <111> components was suppressed in the recrystallized texture near the surface, and the vicinity of the {100}<001> component was developed after grain growth. The relation between RSF and cold-rolling condition was examined by computer simulation; such results were attributed to the increment of shear strain in the surface texture. Magnetic properties would be improved by adequate control of cold-rolling condition.

Keywords cold rolling, cubic orientation, magnetic induction, non-oriented electrical steel, rolling shape factor, texture

1. Introduction

The magnetic properties of non-oriented electrical steel strongly depend on its texture. To improve magnetic properties, it is important to increase the intensity of {100} or {110} texture, which consists of easily magnetized <100> direction on the strip plane, and to decrease that of {111}, which consists of hard magnetized <111> orientation near its plane (Ref 1, 2).

Concerning the texture formation of hot strip, Senuma et al. (Ref 3) showed by calculation that the surface texture is strongly influenced during fabrication by the friction between rollers and the sheet. They confirmed that with decreasing friction, the surface texture of a sheet becomes similar to that of the center.

The texture evolution of cold rolling has been speculated on by Regenet-Stuwe (Ref 4), Dillamore-Roberts (Ref 5), and others. But except for cold rolling reduction, there has been little quantitative analysis (Ref 6) of the material properties such as magnetic induction and the effect of the cold rolling condition. The purpose of the present paper is to reveal the effect of the cold rolling condition on the magnetic properties and the texture of non-oriented electrical steel.

2. Experimental Procedure

The purpose of this experiment was to show that cold rolling reduction and also the condition of each pass affects the magnetic properties of non-oriented electrical steel. So the total cold rolling reduction was the same.

A specimen of electrical steel was prepared by vacuum melting. The chemical composition of the steel was 18 ppm C, 0.26 wt% Si, 0.20 wt% Mn, 3 ppm S, 0.026 wt% sol-Al, and 6 ppm N. The ingots were heated to 1373 K, hot rolled to sheetbar 49 and 63 mm thick, respectively, and cooled. They were cut and reheated to 1423 K and hot rolled to 3.10 and 4.01 mm thick, respectively. The finishing temperature of final hot rolling was 1123 K. They were then pickled and cold rolled.

The cold rolling conditions are shown in Table 1. All specimens received the same 82% reduction. Work roller radii of 30, 60, and 100 mm, respectively, were chosen. For the thickness of hot strip, gages of 3.10 and 4.01 mm were chosen. The grain size of hot strip also strongly affects the texture evolution (Ref 7, 8) during cold rolling and recrystallization, so strips that had almost the same grain sizes were chosen. All specimens were cold rolled for one direction and cooled to room temperature after each pass. No lubricant was used between strip and work roll.

Annealing for recrystallization was conducted at 923 K for 30 s. From these strips, single-sheet test samples were cut and the magnetic properties were measured.

For evaluation of magnetic properties, the B50 of each specimen was measured. This is the value of magnetic induction of materials measured at the exciting current 5000 A/m. In other words, it is a kind of permeability. If core materials possessing higher B50 values are used for motors, higher torque or magnetized force is attained by lower exciting current. Furthermore, core losses caused by copper wire resistance of motors are prevented, and motors can be fabricated in more compact sizes. Consequently, improving the B50 of materials saves energy and materials.

Finally, the specimens were annealed at 923 K for 2 h. The purposes of this annealing were to relieve residual stress caused by fabrication and to improve loss by grain growth (Ref 9). After that, magnetic properties were measured and grain size of specimens was measured by the intersection method using an optical microscope.

Texture was measured with a Rigaku RINT1500 and orientation distribution function (ODFs) were calculated for three-dimensional textures. These calculations were made by the

Table 1 Experimental cold rolling condition

Parameter	Value
Reduction, %	82.0
Radius of work roll, mm	30, 60, 100
Hot strip gage, mm	3.10, 4.01
Cold strip gage, mm	0.55, 0.72
Grain size (hot strip), μm	66.1, 64.6

R. Kawamata, T. Kubota, and **K. Yamada,** Nippon Steel Corp., Steel Research Lab, 20-1 Shintomi Futtsu, Chiba, 293, Japan.

series expansion method ($I_{max} = 22$) (Ref 10) from three complete pole figures of {100}, {110}, and {112}.

Orientation distribution function is the statistical distribution function of crystallographic orientations of crystal grains in the materials. This function has a close relation to B50 data because each crystal grain has easily magnetized orientations as well as orientations that are not as easily magnetized. Therefore the magnetic properties of each grain strongly depend on the crystal orientation distribution. It is well known that if easily magnetized crystal grains are better distributed in ODF, the materials are suitable for magnetic use (Ref 11).

3. Experimental Results

Figure 1 shows the dependence of B50, magnetic induction of annealed specimens, on the cold rolling condition. The data are plotted against the thickness of hot strip. From this figure, three conclusions can be drawn. The first is that magnetic induction increases when the radius of work roller becomes smaller. The second is that magnetic induction increases when hot strip is thicker. The third is that in the two annealed specimens with highest B50, more than 1.79 T (see the left side of Fig. 1), B50 did not vary so much after grain growth by stress relief annealing (see the right side of Fig. 1). On the contrary, the annealed specimens with lower B50 degraded by stress relief annealing (compare the closed square and triangle points in the left side of Fig. 1 and those in the right side).

These facts cannot be attributed to differences in cold rolling reduction. But it can be inferred that heterogeneous deformation during cold rolling has some influence on these phenomena. So, we have to evaluate each pass by some kind of new parameter that can represent the heterogeneity of deformation.

4. Adoption of Rolling Shape Factor for the Evaluation of Cold Rolling

For estimating heterogeneity of deformation during rolling, the rolling shape factor (RSF) has been used in plate rolling (Ref 12). It is defined by:

$$RSF = 2(R(h_1\text{-}h_0))^{0.5}/(h_0 + h_1) \quad \text{(Eq 1)}$$

where R is the radius of work roll and h_0 and h_1 are the thickness of the strip after and before the pass, respectively. This parameter consisted of the projected length of contact divided by the mean thickness of the strip before and after the pass. A large RSF means that the strain distribution induced by rolling is more homogeneous, and on the contrary, a small RSF means that the deformation was more heterogeneous.

5. Computer Simulation of Strain Distribution in the Strip

To estimate the effect of the RSF on the distribution of strain in the strip, computer simulations of several different rolling conditions were made. They were achieved by finite element rigid plastic deformation analysis, named numerical system for computer analysis of rolling mechanism (Ref 13). The calculations were done under plane strain, and the formula of yield stress of the strip was:

$$\sigma y = 62.63\ (\varepsilon + 0.0067)^{0.208} \quad \text{(Eq 2)}$$

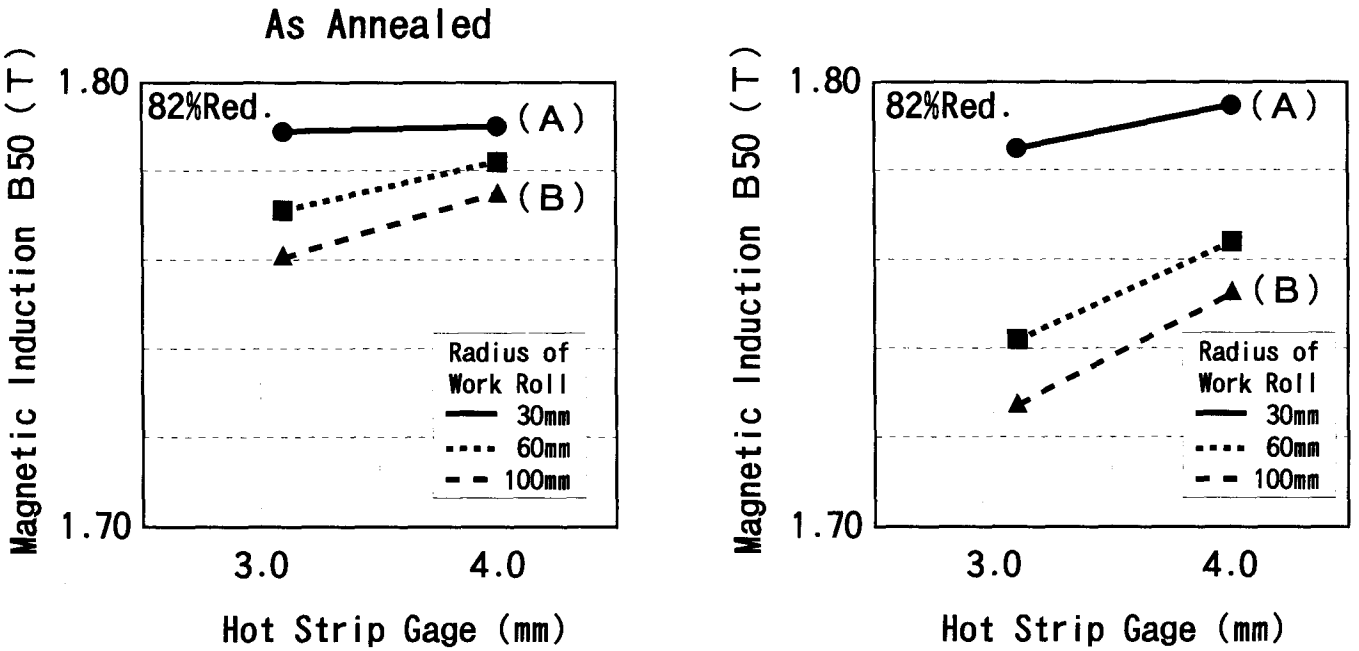

Fig. 1 Dependence of magnetic induction on cold rolling condition

where ε is the equivalent strain ($\varepsilon = \{(2/3)\ \varepsilon_{ij}\ \varepsilon_{ij}\}^{0.5}$) and constants in the formula are identified from the stress-strain curve of a tensile test.

The rolling speed was 100 mm/s and the coefficient of friction between roll and sheet was set at 0.10. To simplify the calculation, the reductions were set at one pass at 28.6%. The conditions of calculations are shown in Table 2. In one condition, the thickness of the strip was held constant but the radius of the work roll was changed, and for the other, the radius of the work roll was held constant while the thickness of the hot strips was changed.

The result is shown in Fig. 2. The equivalent strain is plotted on the horizontal axis, and the position along the thickness is plotted on the vertical axis. Although each calculation was made under the same reduction, distribution of the equivalent strain is quite different. The equivalent strains at the center take the same value, but at the strip surface, when the radius of work roll is smaller, the strain near the surface is larger, and when the gage of strip is thicker, the strain near the surface is larger. The dependence of the equivalent strains on the RSF are shown in Fig. 3. Strain data can well be set in order by RSF.

The equivalent strain is independent of RSF at the center, but near the surface, the smaller the RSF, the larger the equivalent strain. The reason, we assume, is that only compressive deformation occurred at the center, so that the equivalent strain was unchanged, but that near the surface, additional shear deformation occurred and consequently the equivalent strain increased.

From these results, it is clear that RSF has an influential effect on the strain distribution and that as a result, the magnetic properties and texture of products will be affected.

6. Relation between RSF and Magnetic Induction

In the experiment previously noted, RSF was calculated from an average of each pass.

The relation between the B50 value of the annealed specimens and their RSF is shown in Fig. 4. They have good correlation, and B50 values strongly depend on RSF. The B50 value increases when the RSF decreases.

Another noticeable result of this experiment is shown in Fig. 5, which shows the change of the B50 value of each specimen after stress relief annealing. The degradation of the B50 value also depends on the RSF. It degrades in the case of a larger RSF (see B in Fig. 5), but it does not change so much in the case of a smaller RSF (see A in Fig. 5). In other words, specimens that possess a higher B50 value right after annealing degrade little after grain growth by stress relief annealing (see

Table 2 Calculation condition of cold rolling

Drafting schedule (reduction percent)	Radius of work roll, mm	Rolling shape factor
Constant thickness, varied radii of work roll		
2.70 → 1.93 (28.6%)	200	5.37
2.70 → 1.93 (28.6%)	100	3.80
2.70 → 1.93 (28.6%)	30	2.08
Varied thickness, constant radius of work roll		
2.70 → 1.93 (28.6%)	200	5.37
3.70 → 2.64 (28.6%)	200	4.59
4.70 → 3.36 (28.6%)	200	4.07

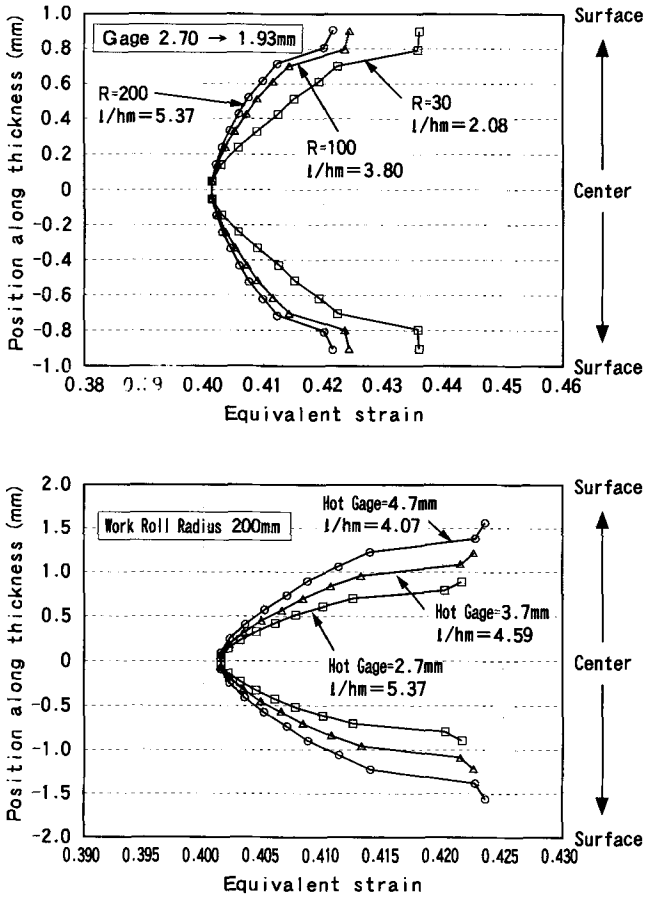

Fig. 2 Calculation results of equivalent strain distribution. Reduction was 82% by one pass.

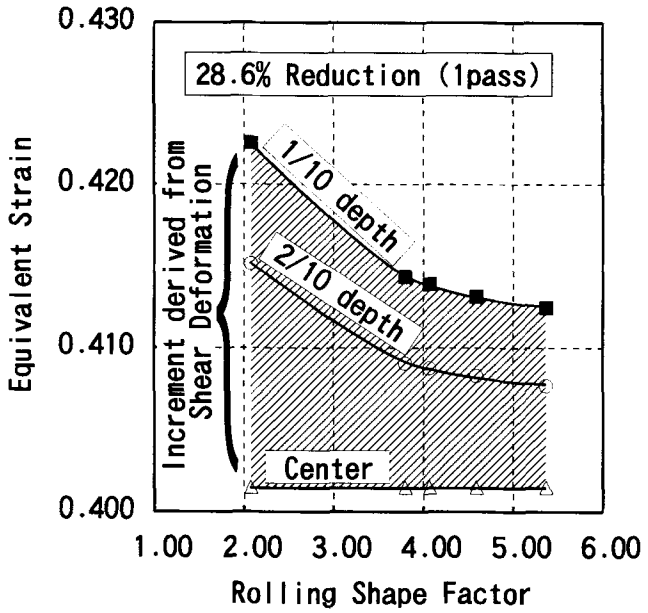

Fig. 3 Dependence of equivalent strain on RSF

A in Fig. 5 and Table 3). Conversely, specimens that possess a lower B50 value right after annealing degrade greatly after stress relief annealing (see B in Fig. 5 and Table 3).

There is a close relation between texture and B50 values (Ref 1, 2, 11), and this implies that RSF affects the texture evolution of non-oriented electrical steel. From the computer simulation of the strain distribution, as noted above, the distribution of equivalent strain increases near the strip surface. This effect is enhanced in the case of a smaller RSF, and texture evolution is strongly affected by strain (Ref 3). So we could infer that changes in magnetic induction are derived mainly from the change of texture near the surface.

To reveal the reason for such changes in magnetic properties, we selected two samples and investigated the texture of both surface and center. The chosen samples are marked with (A) and (B) in Fig. 4 and 5. The average RSF of (A) and (B) are 0.87 and 1.41, respectively. As shown in Table 3, the B50 values of (A) and (B) are 1.791 and 1.775 T after first annealing, respectively, and 1.795 and 1.753 T after stress relief annealing, respectively. The grain size of each specimen is shown in Table 4. The grain sizes of specimens (A) and (B) are almost the same, so the differences of induction and texture between (A) and (B) cannot be attributed to grain size. However, the induction changes of the two specimens after stress relief annealing are quite different. The induction of specimen (B) degrades by 0.022 T after stress relief annealing, while that of specimen (A) slightly increases by 0.004 T. Consequently, the induction of specimen (A) is larger than that of specimen (B) in the case of both annealed and stress-relief annealed specimens.

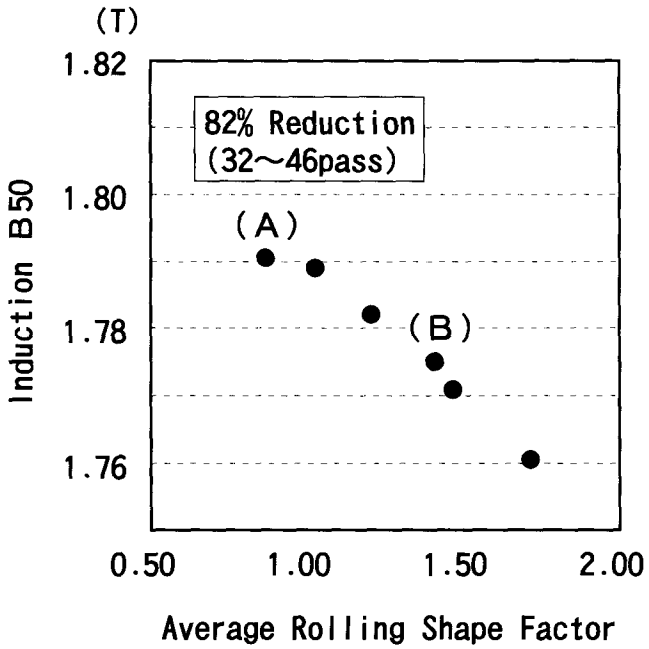

Fig. 4 Dependence of magnetic induction of annealed specimens on RSF

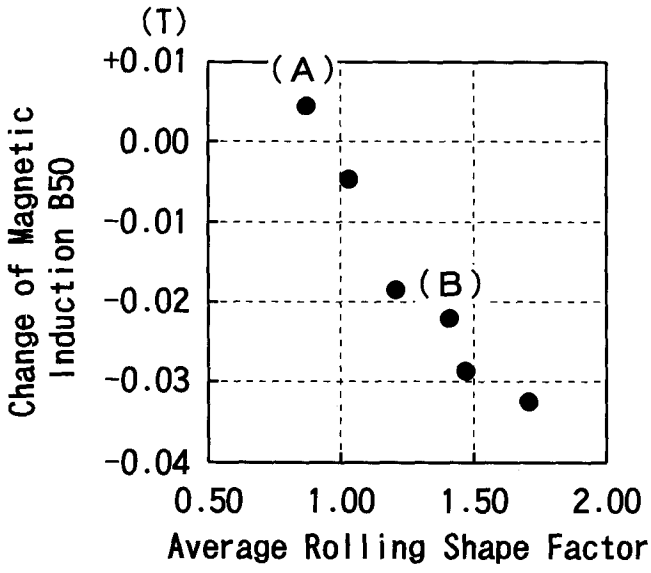

Fig. 5 Dependence of B50 value change, after grain growth by stress relief annealing, on RSF

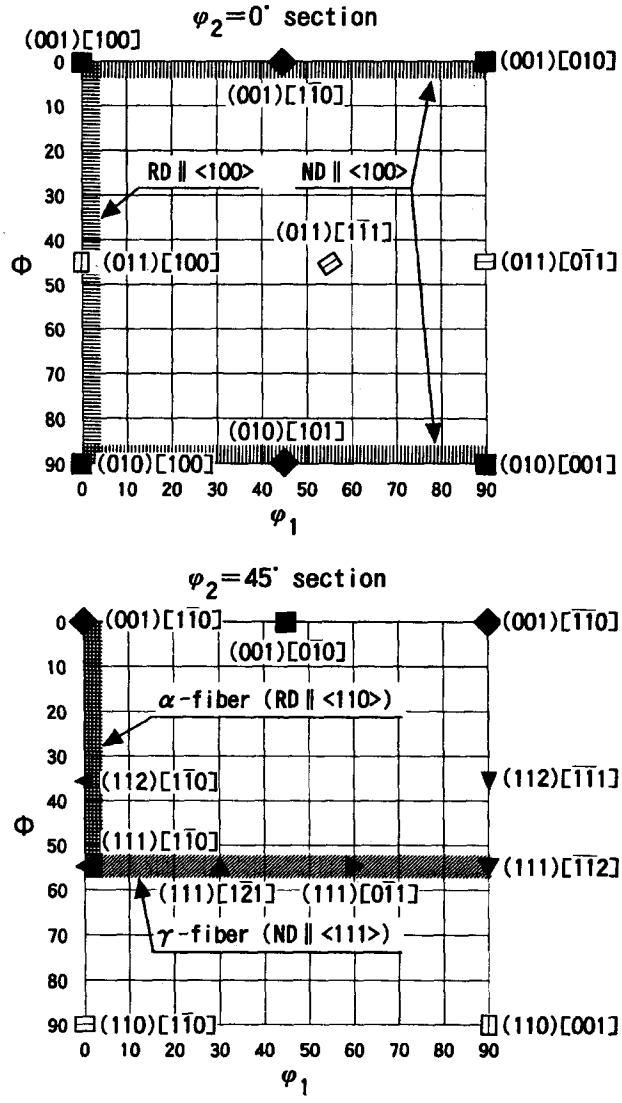

Fig. 6 Orientation distribution of $\varphi_2 = 0°$ and $\varphi_2 = 45°$ sections

Table 3 Magnetic induction of specimens

Parameter	Specimen A	Specimen B
Rolling shape factor	0.87	1.41
B50 after annealing (as-recrystallized), T	1.791	1.775
B50 after stress relief annealing (after grain growth), T	1.795	1.753
B50 change after stress relief annealing, T	+0.004	-0.022

Table 4 Grain size of specimens

Parameter	Specimen A	Specimen B
Rolling shape factor	0.87	1.41
Grain size, annealed (as-recrystallized), μm	13.6	13.2
Grain size, stress-relief annealed (after grain growth), μm	80.6	76.8

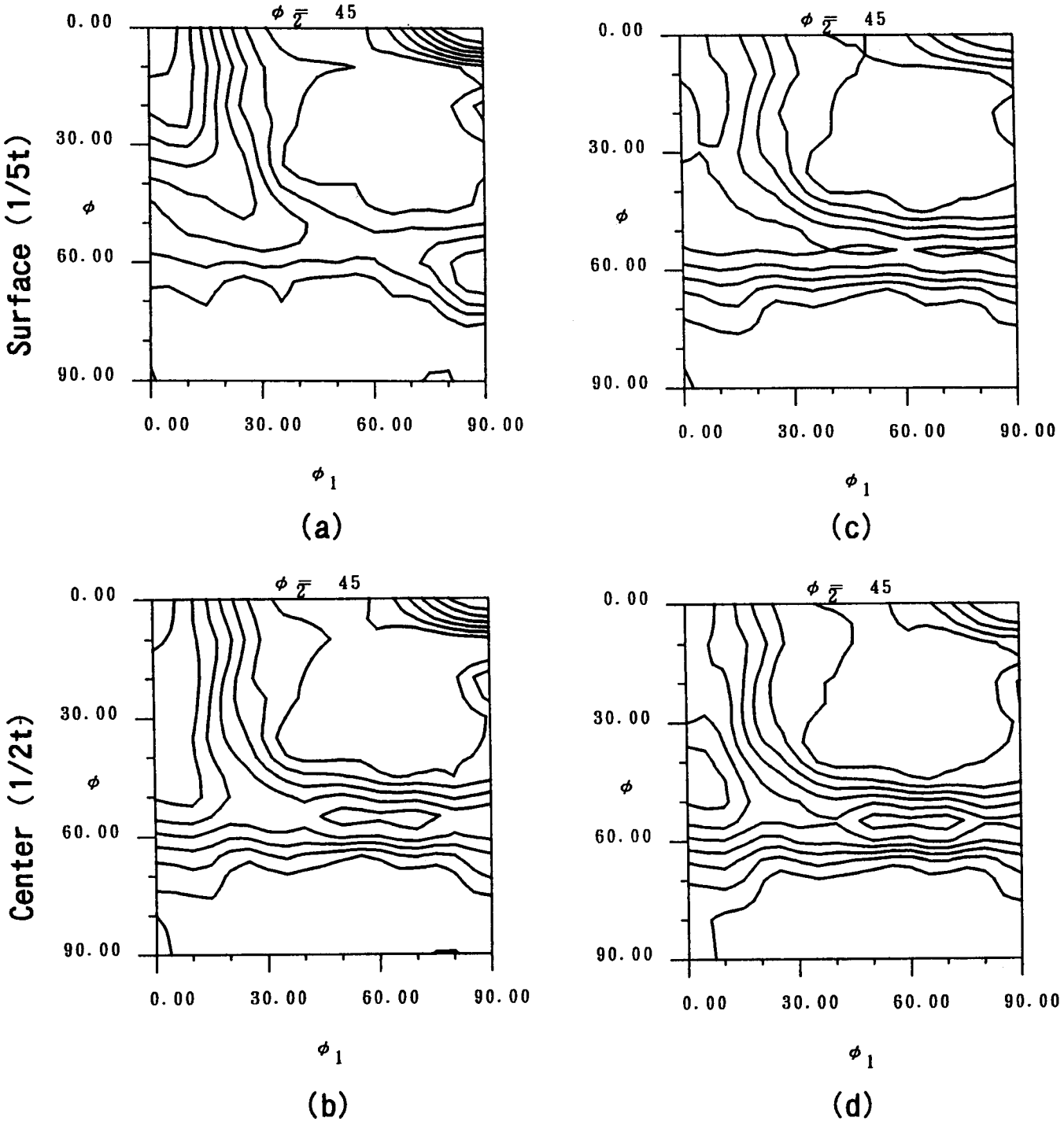

Fig. 7 Cold-rolled texture. $\varphi_2 = 45°$. (a) and (b) Specimen A, RSF = 0.87. (c) and (d) Specimen B, RSF = 1.41. Contour lines are 1-2-3-4-5-6-7-8

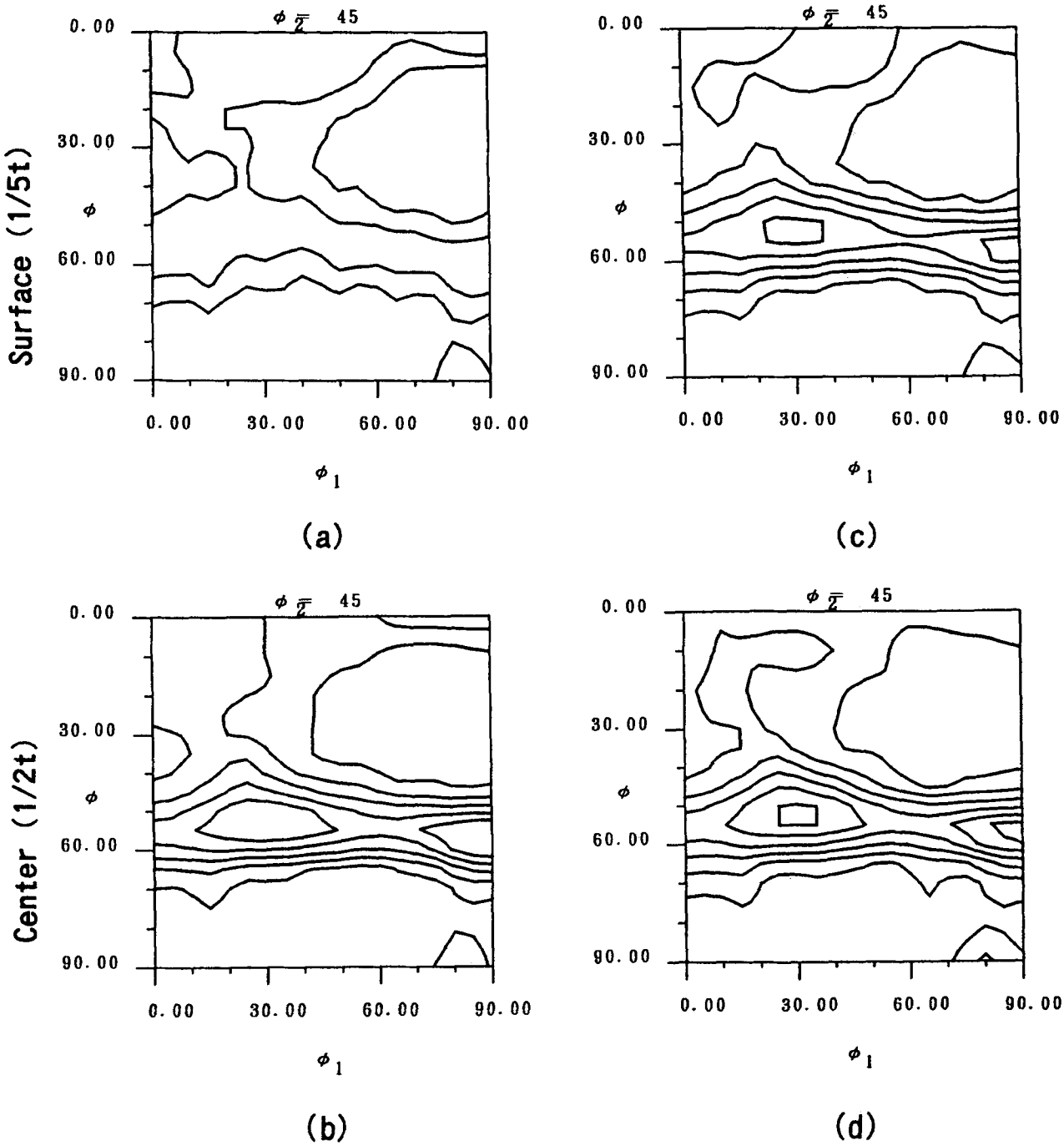

Fig. 8 Annealed texture. $\varphi_2 = 45°$. (a) and (b) Specimen A, RSF = 0.87. (c) and (d) Specimen B, RSF = 1.41. Contour lines are 1-2-3-4-5-6

7. Textures

7.1 *Cold-Rolled Texture*

The locations of each orientation component for the $\varphi_2 = 0°$ and $\varphi_2 = 45°$ sections of Euler space are shown in Fig. 6 (Ref 14). In Fig. 6, ND || <100> components and RD || <100> components, the most easily magnetized crystal orientation components, are shows by vertically and horizontally hatched areas, respectively, in the $\varphi_2 = 0°$ section figure. The $\varphi_2 = 45°$ section figure shown ND || <111> components, namely γ fiber, which is rotating around the <111> crystal axis perpendicular to the sheet plane, possessing nearly the least easily magnetized crystal orientation on the sheet plane, and RD || <011> components, namely α fiber, which is rotating around the crystal axis of RD || <011> from (001)[1$\bar{1}$0] to (111)[1$\bar{1}$0], shown by obliquely and cross-hatched areas, respectively.

Figure 7 shows the ODF by the Bunge method (Ref 14) of cold-rolled specimens. They are on the section of $\varphi_2 = 45°$. In the specimen with a smaller RSF, the development of α fiber, RD || <011> is weaker than that of the specimen with a larger RSF. The surface texture of specimen (A) in Fig. 7(a) is differ-

ent from that of the others. The main component has a {100} <011> orientation, but the others have a {211} <011> orientation.

7.2 *Recrystallized Texture by Annealing*

Figure 8 shows the ODF of annealed specimens. They are on the section of $\varphi_2 = 45°$. Figures 8(b), (c), and (d) show the developed γ fiber, ND ∥ <111> textures. Their main component is {111} <112> with more than 5.0×. On the other hand, γ fiber is suppressed near the surface of specimen (A) in Fig. 8(a). At the surface of specimen (A), the main component exists in the section of $\varphi_2 = 0°$. It is shown in Fig. 9. Its intensity is only 3.0× and its orientation is {610} <001>.

7.3 *Grain Growth Texture by Stress Relief Annealing*

Figure 10 shows the ODF of stress-relief annealed specimens. They are on the section of $\varphi_2 = 45°$.

With stress relief annealing, the differences between the textures of the specimens are more distinct. The difference is especially clear near the surface of the specimens. After grain growth by stress relief annealing, in the case of Fig. 10(b), (c), and (d), the γ fiber intensity increases to 8.0 to 9.0× and the main component is {111} <112>. However, in the case of specimen (A), its main component is shown in Fig. 11 and its orientation is {410} <001>, while the intensity of γ fiber is much lower than that of the others (Fig. 10a).

8. Relation between Texture and Magnetic Induction

These results can be summarized as follows: in the case of a large RSF, as in specimen (B), the surface texture as well as the midplane texture develops γ fiber, that is, ND ∥ <111> texture, and its main component is {111} <112>. Furthermore, with grain growth by stress relief annealing, its intensity is increased. The orientation {111} <112> has the <112> axis on the sheet plane, and it is close to the hard magnetization orientation of <111> (Ref 1), so that increments of ND ∥ <111> texture cause the degradation of induction after stress relief annealing.

On the other hand, in the case of a small RSF, specimen (A), the accumulation of ND ∥ <111> texture is suppressed near the surface, both annealed recrystallization texture and grain growth texture by stress relief annealing. The main components of texture are {610} <001> and {410} <001>, respectively, which consists of one component of easily magnetized <100> axis on the rolling direction and of another one of <010> slightly inclined from the strip plane, so that the surface texture of a small-RSF specimen has two easily magnetized <001> orientations on its sheet plane. As a result, in spite of increments of ND ∥ <111> texture at the midplane, B50 values are not changed in specimen (A) after grain growth by stress relief annealing.

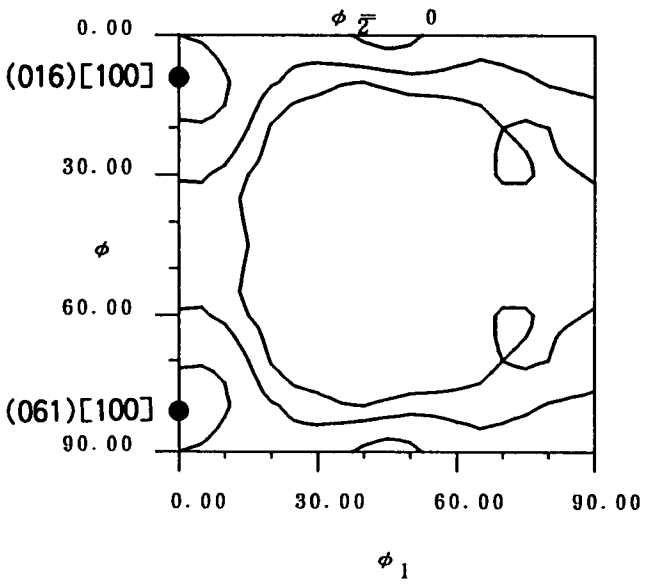

Fig. 9 Annealed texture in the surface (1/5 thick). $\varphi_2 = 0°$. Specimen A, RSF = 0.87. Contour lines are 1-2-3

9. Consideration of Texture Formation

We pointed out above that RSF can be used for indices for evaluating the effect of cold rolling condition on magnetic properties, and that alteration of the distribution of the strains near the strip surface is the reason for such changes in magnetic properties.

9.1 *Difference of Rolling Texture Formation*

First, we will examine the differences in surface texture development of cold-rolled specimens. In the low-RSF samples, the development of RD ∥ <011>, so-called α fiber, is weak and {100} <011> is instead the main component (see Fig. 7a). On the other hand, high-RSF samples showed the development of RD ∥ <011> fiber and ND ∥ <111> fiber texture, and {211} <011> is recognized as the main component (see Fig. 7c, d). These changes of rolling texture formation might be caused by cross slip during deformation. In high reduction of body-centered cubic metal, Dillamore and Roberts studied the texture formation mechanism and concluded that cross slip enhances the deviation of rolling texture from {211} <011> to {100} <011> (Ref 5). In this case, it is assumed that the additional strain caused by shear deformation near the strip surface might enhance the cross slip and consequently, {110} <001> becomes the main component in lower-RSF specimens.

9.2 *Formation of Recrystallization Texture*

Some people insist that cold-rolled and recrystallized textures have a special relationship that consists of rotation around a certain axis. For example, recrystallized {111} <112> has the relation with cold-rolled {211} <011> of rotating around the <011> axis by about 35° (Ref 15).

Another view is that surface recrystallization texture of low RSF does not have an orientation relation with cold-rolled texture. The intensity of each component in ODF is weak and its

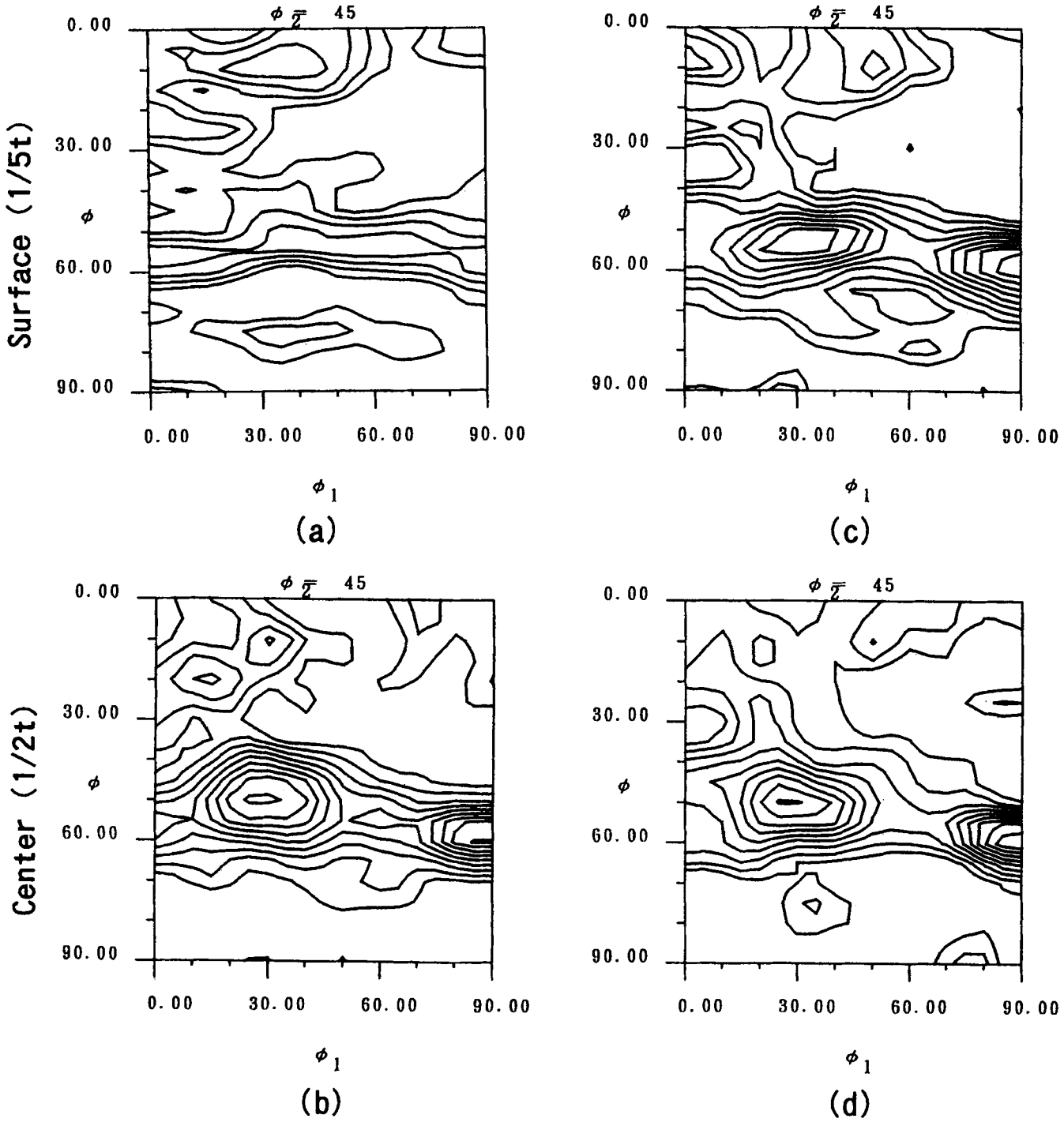

Fig. 10 Stress-relief annealed texture. $\varphi_2 = 45°$. (a) and (b) Specimen A, RSF = 0.87. (c) and (d) Specimen B, RSF = 1.41. Contour lines are 1-2-3-4-5-6-7-8-9

texture shows rather random orientation distribution. For example, its maximum intensity is only 3.0× less than 60% of the maximum intensity of the main components of other specimens, which is more than 5.0×.

There are several possibilities for the formation mechanism of this recrystallized texture. One is that there exist near-cubic nuclei that possess higher stored energy in the deformed matrix, for example within shear bands, and that they grow into a {100} <011> matrix.

Another possibility is to assume that orientation of nucleus is supposed to be rather random because of complicated strain, so that grains of high coincident boundary with matrix orientation could be selected to grow. Actually, a bit deviated {100} <011>, that is, {611} <011> has a Σ5 relationship, which is rotating 36.87° around the <010> axis, with {610} <001>. But the physical meaning of such rotation is not clear.

Also, after grain growth, the main component in the surface texture of a small-RSF specimen is slightly rotated around the

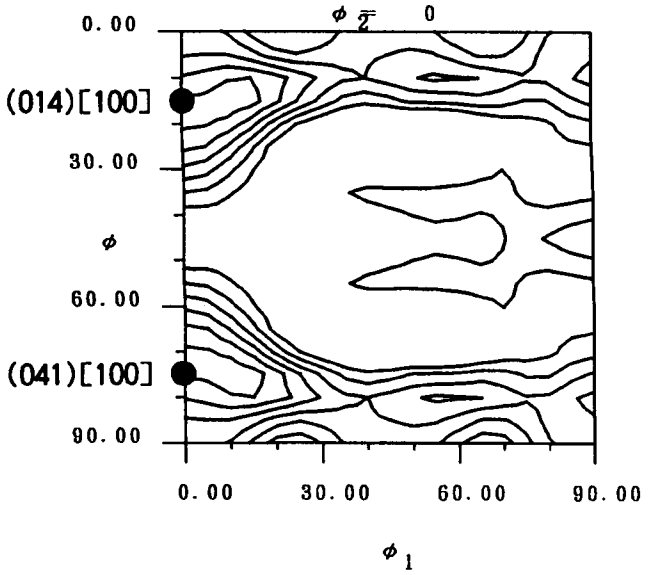

Fig. 11 Stress-relief annealed texture in the surface (1/5 thick). $\varphi_2 = 0°$. Specimen A, RSF = 0.87. Contour lines are 1-2-3-4-5-6

<001> axis from {610} <001> to {410} <001>, and its intensity is also increased. This causes the stability of B50 values during stress relief annealing.

We need more study to reveal the reason why the vicinity of just cubic orientation becomes the main component in the recrystallized and grain growth texture on the surface of lower-RSF specimens.

10. Conclusions

We have demonstrated that the RSF is a useful parameter for conveniently evaluating the relation between the cold rolling condition and magnetic properties, and we have evaluated the influence of RSF on magnetic induction quantitatively. In the present study, the magnetic properties of non-oriented electrical steel were especially affected by the surface texture evolution.

- The RSF can be used to evaluate the effect of cold rolling on the magnetic properties of non-oriented electrical steel.
- In case of small RSF of cold rolling, shear strain increases near the strip surface.
- When RSF is small, near the surface of a specimen, the development of ND ∥ <111> texture is suppressed and the main component becomes the vicinity of just cubic orientation in both recrystallization and grain growth texture.
- The improvement of magnetic properties by changing the RSF stems from surface texture change.

References

1. K. Honda and S. Kaya, *Sci. Rep. Tohoku Univ.*, Vol 15, 1926, p 721
2. H.J. Williams, *Phys. Rev.*, Vol 52, 1937, p 747
3. T. Senuma, H. Yada, G. Matsumura, and K. Yamada, *Tetsu-to-Hagané*, Vol 73, 1987, p 1598-1605
4. P.J. Regenet and H.P. Stuwe, *Z. Metallkd.*, Vol 54, 1963, p 273
5. I.L. Dillamore and W.T. Roberts, *J. Inst. Met.*, Vol 92, 1963/64, p 193
6. H. Murakami, Y. Huruno, and T. Kawano, *CAMP-ISIJ*, Vol 5, 1992, p 902
7. M. Matsuo, S. Hayami, and S. Nagashima, *Proc. Int. Conf. on the Science and Technology of Iron and Steel, Trans. ISIJ*, Part II, 1971, p 867
8. M. Abe, Y. Kokabu, Y. Hayshi, and S. Hayami, *J. Jpn. Inst. Met.*, Vol 44, 1980, p 84-94
9. K. Ueno, I. Tachino, and T. Kubota, *Metallurgy of Vacuum-Degassed Steel Products*, R. Pradhan, Ed., The Minerals, Metals and Materials Society, PA, 1990
10. H.J. Bunge, *Texture Analysis in Materials Science*, Butterworths, London, 1982
11. I. Tachino, *Tetsu-to-Hagané*, Vol 81, 1990, p 81-88
12. N. Okumura, T. Kubota, M. Nagumo, J. Hada, and A. Saito, *Proc. Int. Conf. on Steel Rolling*, Part I, Iron and Steel Institute of Japan, Tokyo, 1980, p 217-228
13. K. Yamada, S. Ogawa, and M. Ataka, *Proc. Fourth Int. Conf. on Numerical Methods in Industrial Forming Processes*, Balkema, Rotterdam, 1992, p 755
14. H.J. Bunge, *Z. Metallkd.*, Vol 56, 1965, p 378, 872
15. T. Urabe and J.J. Jonas, *ISIJ Int.*, Vol 34, 1994, p 435-442